A Spectral Approach to Nondestructive Testing via Electromagnetic Waves

Fioralba Cakoni[(a)], Samuel Cogar[(a)] and Peter Monk[(b)]

Abstract—**In recent years a new approach has been proposed in the study of the inverse scattering problem for electromagnetic waves. In particular, a study is made of the analytic properties of the scattering operator and the results of this study are used to design target signatures that respond to changes in the electromagnetic parameters of the scattering medium. These target signatures are characterized by novel eigenvalue problems such that the eigenvalues can be determined from measured scattering data. Changes in the structural properties of the material or the presence of flaws cause changes in the measured eigenvalues. In this paper we provide a general framework for developing target signatures, and numerical evidence of the efficacy of new target signatures based on recently introduced eigenvalue problems arising in electromagnetic scattering theory for anisotropic media.**

Index Terms—**Electromagnetic scattering, inverse problems, target signature, Stekloff eigenvalues, modified transmission eigenvalues.**

I. INTRODUCTION

INVERSE scattering theory is central to such diverse areas of application as medical imaging, geophysical exploration and nondestructive testing. Typically the inverse scattering problem is both nonlinear and ill-posed, thus presenting particular difficulties in the development of efficient inversion algorithms. Many existing algorithms are based on either a weak scattering approximation (linearization) or on the use of nonlinear optimization techniques. Nonlinear optimization can successfully determine full details of a scatterer (even when the scattering is not weak) in many cases and is very flexible. Despite strong progress on algorithms [1]–[6] and theory [7] for this problem, it is still computationally intensive.

An alternative class of approaches, termed *qualitative methods*, attempts to use more extensive data to reduce computational cost while still avoiding the weak scattering assumption. The target signature algorithms we shall describe here are motivated by our study of a particular qualitative method called the Linear Sampling Method (LSM) (see [8], [9] and references therein for

(a) Department of Mathematics, Rutgers University, Piscataway, NJ 08854, USA.
(b) Department of Mathematical Sciences, University of Delaware, Newark DE 19716, USA.

background on the electromagnetic LSM, and [10] for recent progress). Approaches of the type considered here originates in the work of Audibert et al. for the Helmholtz equation [11].

The motivation for proposing target signatures in nondestructive testing is twofold. First there are some problems that are not amenable to existing methods of interrogation based on linearization or optimization, and second it may be desirable to have a relatively simple method for the classification of scatterers.

As an example of the first case, airplane canopies can suffer degradation from continuous exposure to ultraviolet radiation from sunlight. The degradation takes the form of the weakening of the polymer structure of the canopy. It would therefore be useful if these canopies could be quickly and simply inspected so that replacements were not ordered earlier than needed. In such a problem complications arise due to the fact that in general the spatially varying permittivity and conductivity tensors of the material being tested are anisotropic, thus not uniquely determined from any amount of scattering data unless a specific structure is assumed (c.f. [12] for the Helmholtz case). In spite of this complication one would nevertheless like to test for either structural changes in the material or the presence of voids or cavities. One approach for doing this might be to identify certain discrete "target signatures" characterized by novel eigenvalue problems such that these eigenvalues can be determined from the measured scattering data. Changes in the structural properties of the material or the presence of voids or cavities can then potentially be detected by changes in the measured eigenvalues. In our investigation the shape of the inhomogeneity is known, since it represents the object being evaluated. In addition, changes in the structural properties of the object are identified without making use of the governing equations that model the healthy material. Therefore our approach, although presented here at a conceptual level, could be adapted to specific problems of monitoring structural integrity of a complicated material for which a precise model is not available.

Another situation where target signatures may be of use is in the classification of scatterers. This is not a nondestructive testing application, but possibly knowledge of

target signatures could be used to identify the scatterer from a predefined dictionary. Indeed this is the original intent of the Singularity Expansion Method (SEM) pioneered by Baum [13] (see also [14]).

In this paper we shall consider the simple case of a scatterer in free space as proof-of-concept. It is possible to consider more complicated background media, and conceptually the theoretical discussion will remain the same; however, we choose this simple case to avoid technicalities in our presentation. Obviously much more work needs to be done to adapt the method to any specific problem in nondestructive testing. We note that in the acoustic context some progress has been made in using target signatures to determine crack density in solids [15]. Extensions of electromagnetic target signatures in this direction would be worthwhile.

The novelty of this paper is twofold: first we present a general framework for constructing target signatures using eigenvalue problems, and second we test one such method on some basic test problems.

The paper is arranged as follows: in the next section we summarize the forward scattering problem for Maxwell's equations to fix notation and the context of our study. Then in Section III we discuss a general approach to obtaining target signatures. We also give two examples: Steklov type target signatures, and modified interior transmission eigenvalues. Finally in Section IV we present some numerical results for the latter class of eigenvalues.

II. SCATTERING BY AN INHOMOGENEOUS MEDIUM

We consider time harmonic electromagnetic waves propagating in a medium occupying the whole space $\mathbb{R}^3$ with tensor electric permittivity ϵ, magnetic permeability μ and electric conductivity σ. With ϵ_0 and μ_0 denoting the permittivity and permeability of free space, the relative permittivity, permeability, and conductivity are given by

$$\epsilon_r(x) := \epsilon(x)/\epsilon_0, \ \mu_r(x) := \mu(x)/\mu_0,$$

and $\sigma_r(x) := \sqrt{\mu_0/\epsilon_0}\sigma(x)$. Denoting by ω the angular frequency of the radiation, the wave number is $k > 0$ defined by $k^2 = \epsilon_0\mu_0\omega^2$,

With this notation, if $J(x)$ is the current density, the complex-valued electric field $E(x)$ and magnetic field $H(x)$ satisfy the time-harmonic *Maxwell's equations*

$$\text{curl } E - ik\mu_r H = 0, \ \text{curl } H + ik\epsilon_r E = J \text{ in } \mathbb{R}^3, \ (1)$$

where, by Ohm's law, $J(x) = \sigma_r E(x)$. In this case the full time domain electric and magnetic fields ($\mathcal{E}$ and $\mathcal{H}$ respectively) are given by

$$\mathcal{E}(x,t) = \sqrt{\epsilon_0}\Re(E(x)e^{-i\omega t}),$$
$$\mathcal{H}(x,t) = \sqrt{\mu_0}\Re(H(x)e^{-i\omega t}).$$

We assume the existence of a (possibly anisotropic) inhomogeneity, here referred to as the target, occupying a region D which is a bounded simply connected subdomain of $\mathbb{R}^3$ and has piece-wise smooth boundary ∂D with ν the unit outward normal vector. The relative electric permittivity $\epsilon_r(x)$, magnetic permeability $\mu_r(x)$ and electric conductivity $\sigma_r(x)$ for $x \in D$ are allowed to be matrix-valued functions with bounded entries with the property that, for all $\xi \in \mathbb{R}^3$,

$$\xi \cdot \epsilon_r(x)\xi \ge \alpha\|\xi\|^2, \ \xi \cdot \mu_r(x)\xi \ge \beta\|\xi\|^2, \ \xi \cdot \sigma_r(x)\xi \ge 0$$

with some constants $\alpha > 0$, $\beta > 0$, and for almost all $x \in D$. For simplicity of this presentation, we assume that the above inhomogeneity D is situated in a homogeneous dielectric background. Thus in $\mathbb{R}^3 \setminus \overline{D}$, we have electromagnetic parameters given by constants $\epsilon_r = 1$, $\mu_r = 1$ and $\sigma_r = 0$.

The inhomogeneity is probed by incident electromagnetic fields $\mathcal{E}^i(x,t)$ and $\mathcal{H}^i(x,t)$ that in general are solutions to the background Maxwell's equations. Although more general sources can be used (e.g. point sources), to fix our ideas, we consider interrogating with a time harmonic electric plane wave

$$E^i := \frac{i}{k} \text{ curl curl } p \, e^{ikx \cdot d}, \ H^i := \frac{1}{ik} \text{curl } E^i, \quad (2)$$

where $d \in \mathbb{R}^3$ is a unit vector giving the direction of propagation and $p \in \mathbb{R}^3$, $p \ne 0$, is the polarization vector.

Using our assumption of a bounded scatterer, we see that the equations governing the time-harmonic electromagnetic wave propagation in the background are

$$\text{curl } E - ikH = 0, \ \text{curl } H + ikE = 0, \quad (3)$$

whereas in D we see from (1) that E and H satisfy

$$\begin{cases} \text{curl } E - ik\mu_r(x)H = 0 \\ \text{curl } H + ik\left(\epsilon_r(x) + \frac{i}{k}\sigma_r(x)\right)E = 0. \end{cases} \quad (4)$$

The time-harmonic scattered fields E^s and H^s satisfy the background equations (3) in the exterior of D and are outgoing, i.e. satisfy the Silver-Müller radiation condition

$$\lim_{|x| \to \infty} |x| \left(\sqrt{\mu_0}H^s \times \hat{x} - \sqrt{\epsilon_0}E^s\right) = 0$$

uniformly with respect to $\hat{x} = x/|x|$. Across the interface ∂D, the tangential components of the total field $E_0 = E^s + E^i$, $H_0 = H^s + H^i$ in $\mathbb{R}^3 \setminus \overline{D}$, and the total field E, H in D satisfying (4) are continuous, i.e.

$$\nu \times E_0 = \nu \times E, \ \nu \times H_0 = \nu \times H \text{ on } \partial D.$$

After eliminating magnetic fields, the scattering problem for the time harmonic electric fields reads: Given the incident field $E^i := E^i(x; d, p, k)$, find $E^s :=$
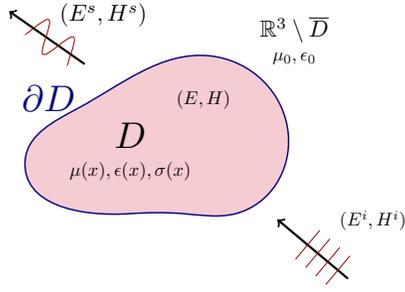
Fig. 1. A cartoon of the direct electromagnetic scattering problem for inhomogeneous media. The known incident field E^i, H^i impinges on the inhomogeneous scatterer occupying the domain D. This creates a scattered field E^s, H^s outside D and a total field E, H in D. The unit normal vector ν points outwards from D.

$E^s(x; d, p, k)$ in $\mathbb{R}^3 \setminus \overline{D}$ and $E := E(x; d, p, k)$ in D such that

$$\operatorname{curl}\operatorname{curl} E^s - k^2 E^s = 0 \qquad \text{in } \mathbb{R}^3 \setminus \overline{D}$$

$$\operatorname{curl} \mu_r^{-1} \operatorname{curl} E - k^2 \left(\epsilon_r + \tfrac{i}{k}\sigma_r\right) E = 0 \quad \text{in } D$$

$$\nu \times E = \nu \times (E^s + E^i) \qquad \text{on } \partial D \quad (5)$$

$$\nu \times \mu_r^{-1} \operatorname{curl} E = \nu \times (\operatorname{curl} E^s + \operatorname{curl} E^i) \quad \text{on } \partial D$$

$$\lim_{|x| \to \infty} \left(\operatorname{curl} E^s \times x - ik|x|E^s\right) = 0.$$

Under the assumptions we have made about the data for this problem, it is possible to show that the problem is well-posed in standard energy spaces (see for example [16]). Once this is done, we see that because E^i depends on d and p we may write $E^i := E^i(x; d, p)$. The scattered field also depends on x, d and p, so $E^s := E^s(x; d, p)$ in $\mathbb{R}^3 \setminus \overline{D}$ and in the same way $E := E(x; d, p)$ in D.

It is known (c.f. [18]) that the outgoing scattered electric field E^s has the asymptotic behavior

$$E^s(x; d, p) = \frac{e^{ik|x|}}{|x|} \left\{ E_\infty(\hat{x}; d, p) + O\left(\frac{1}{|x|}\right) \right\}$$

as $|x| \to \infty$ uniformly with respect $\hat{x} = x/|x|$. The tangential function $E_\infty(\hat{x}; d, p)$ defined on the unit sphere $\mathbb{S}^2$ is the *far field pattern* of the scattered field, and we assume that $E_\infty(\hat{x}; d, p)$ is known (in practice, measured) for all $\hat{x}, d \in \mathbb{S}^2$. Real measurements would be for discrete incoming directions and polarizations, and discrete measurement directions. This is also true for our numerical tests in Section IV.

Our interest in this paper will be in the *inverse scattering problem* where, from a knowledge of $E_\infty(\hat{x}; d, p)$ for $\hat{x}, d \in \mathbb{S}^2$ and two linearly independent polarizations p tangential to $\mathbb{S}^2$ (here referred to as *scattering data*) we seek to find information about $\epsilon_r(x), \mu_r(x), \sigma_r(x)$ for $x \in D$. We remark that the scattering data, even known for all wave numbers k, does not determine uniquely

the matrix-valued coefficients $\epsilon_r, \mu_r, \sigma_r$ that are general functions of position, due to the possibility of transforming the interior of D, leaving the boundary fixed, but distorting the coefficients while having exactly the same scattered field. Thus, in this case, any inverse scattering method would fail to reconstruct these coefficients.

Our inversion approach circumvents this difficulty by providing easily computable target signatures for changes in the reference values of electromagnetic parameters corresponding to an undamaged material instead of recovering any of the coefficients $\epsilon_r, \mu_r, \sigma_r$. More importantly, this is done without the need to know the actual values of the electromagnetic parameters of the healthy inhomogeneity being evaluated. Our target signatures are designed to work for anisotropic, conducting and dispersive electromagnetic materials.

In our investigation of the inverse scattering problem a primary tool will be the *far field operator* (known otherwise as the relative scattering operator) $F : L^2_t(\mathbb{S}^2) \to L^2_t(\mathbb{S}^2)$ defined for $g \in L^2_t(\mathbb{S}^2)$ by

$$(Fg)(\hat{x}) := \int_{\mathbb{S}^2} E_\infty(\hat{x}; d, g(d)) \, ds(d), \qquad (6)$$

where $L^2_t(\mathbb{S}^2)$ is the space of square-integrable tangential fields on $\mathbb{S}^2$. We note that F is a linear compact operator. Clearly Fg is the far field pattern of the scattered field corresponding to the incident field being an *electric Herglotz wave function* with kernel g defined by

$$E_g(x) := \int_{\mathbb{S}^2} e^{ikx \cdot d} g(d) \, ds(d) \qquad g \in L^2_t(\mathbb{S}^2). \quad (7)$$

Note that E_g is a linear superposition of electric plane waves. The study of mathematical properties of the far field operator F, or its modifications, introduces different set of eigenvalues for partial differential operators related to the scattering medium. These eigenvalues, which can be determined from scattering data, are the bases of our target signatures that we develop in the next section.

III. SPECTRAL VALUES AS TARGET SIGNATURES

Spectral properties of operators associated with scattering phenomena carry essential information about the scatterer, and may be useful provided such spectra can be determined from the measured scattering data. As an example, the theory of scattering resonances is a rich and beautiful part of scattering theory (see [14] for a comprehensive survey). However, this theory has not been fruitful in applications even though considerable effort was spent in the past on the related SEM [13] which attempted to use such poles as a method for the target identification of aircraft. In particular, this effort proved to be problematic due to the difficulty of accurately determining these complex wave numbers from measured scattering data.

More recently it was suggested to use *transmission eigenvalues* as target signatures [17], [18]. It is known that the transmission eigenvalue problem is inherent to the scattering phenomena [18]. However, they can only be determined from scattering data for dielectric objects and require broadband data. The newer eigenvalue problems we present here can work at a single fixed frequency and, in principle, for conducting media, although no tests have been preformed yet for such a medium.

Since transmission eigenvalues have been studied for some time (see [19]) we will not discuss them here but acknowledge that the methods presented here are motivated by them. In particular, our approach leads to the *modified transmission eigenvalue problem* and associated target signatures discussed in Section III-C.

The simplest choice of target signature would be eigenvalues of the far field operator, but the connection between such eigenvalues and the properties of the scatterer is not as evident as for the eigenvalues we shall consider [20].

A. Modified Far Field Operators and New Sets of Eigenvalues

The main idea behind modifying the far field operator, and hence obtaining a new class of target signatures, lies in the simple fact that the physical total field $E := E^s + E^i$ corresponding to the scattering problem (5) can be rearranged as $E = (E^s - Q^s) + (Q^s + E^i)$ where Q^s is the scattered field for a fictitious scatterer (to become precise later) due to the incident plane wave E^i (2). Thus, if we now probe by the total field of this fictitious scatterer $Q^s + E^i$, in order to obtain the measured physical total field the response of the scatterer should be $E^s - Q^s$. This means that we can view the total field measurements as coming from our electromagnetic inhomogeneity situated in an artificially changed background interrogated by the total field due to this background. Rewriting the above in terms of the far fields lead to a modified far field operator.

More precisely, let $Q_\infty^\lambda(\hat{x}; d, p, k)$ be the electric far field corresponding to an auxiliary electromagnetic scattering problem (to become precise later) due to the electric plane waves E^i (2) as incident field, and assume that this auxiliary scattering problem depends on a varying parameter $\lambda \in \mathbb{C}$. We denote by $F_\lambda^b : L_t^2(\mathbb{S}^2) \to L_t^2(\mathbb{S}^2)$ the corresponding far field operator

$$(F_\lambda^b g)(\hat{x}) := \int_{\mathbb{S}^2} Q_\infty^\lambda(\hat{x}; d, g(d)) \, ds(d). \qquad (8)$$

Note that the scattering data is only needed at a fixed frequency. We define the *modified far field operator* $\mathcal{F}_\lambda$:

$L_t^2(\mathbb{S}^2) \to L_t^2(\mathbb{S}^2)$ by

$$\mathcal{F}_\lambda g := Fg - F_\lambda^b g. \qquad (9)$$

We emphasize that F is known from the measurements of scattering data at the fixed frequency, whereas F_λ^b is precomputed by solving the chosen artificial scattering problem for a range of $\lambda \in \mathbb{C}$ which does not involve any information on the electromagnetic properties of the medium under interrogation. As we shall see in the next two subsections, the analysis of $\mathcal{F}_\lambda$ yields new eigenvalue problems with $\lambda \in \mathbb{C}$ as the eigenvalue parameter. These in turn can be used as target signatures.

B. Steklov eigenvalues

To explain how a new eigenvalue problem arises from the mathematical properties of $\mathcal{F}_\lambda$ we discuss first a simple auxiliary scattering problem that yields the Steklov eigenvalue problem. To this end, we further specialize $\Omega \subset \mathbb{R}^3$ to be a simply connected region with smooth boundary $\partial\Omega$ such that $D \subseteq \Omega$, and let $Q_\infty^\lambda(\hat{x}, d, p)$ be the far field pattern for the scattering problem with artificial impedance boundary condition:

$$\begin{aligned} \operatorname{curl}\operatorname{curl} Q^s - k^2 Q^s = 0 & \quad \text{in } \mathbb{R}^3 \setminus \overline{\Omega} \\ Q = Q^s + E^i(\cdot; d, p) & \quad \text{in } \mathbb{R}^3 \setminus \overline{\Omega} \\ \nu \times \operatorname{curl} Q - \lambda \nu \times (Q \times \nu) = 0 & \quad \text{on } \partial\Omega \quad (10) \\ \lim_{|x| \to \infty} (\operatorname{curl} Q^s \times x - ik|x|Q^s) = 0. \end{aligned}$$

To see how the modified far field operator gives rise to an eigenvalue problem, we study the injectivity of the corresponding modified far field operator. If $\mathcal{F}_\lambda g = 0$, by Rellich's Lemma [18] we have that $E_g^s \equiv Q_g^s$ in $\mathbb{R}^3 \setminus \Omega$, where E_g^s and Q_g^s are the scattered fields of (5) and (10), respectively, with special incident field $E^i = E_g$ the electric Herglotz wave function (7). Continuity of the tangential components of the total field $E := E^s + E_g$ and $\operatorname{curl} E$ across $\partial\Omega$ along with the boundary condition (10) for $Q_g^s + E_g$ now imply that the function $W := E_g^s + E_g|_\Omega$ satisfies the Steklov eigenvalue problem for Maxwell's equations in Ω

$$\begin{aligned} \operatorname{curl} \mu^{-1} \operatorname{curl} W - k^2 \left(\epsilon_r + \tfrac{i}{k}\sigma_r\right) W = 0 & \quad \text{in } \Omega \\ \nu \times \mu^{-1} \operatorname{curl} W - \lambda \nu \times (W \times \nu) = 0 & \quad \text{on } \partial\Omega. \end{aligned}$$

Thus, if this homogenous problem has only the solution $W = 0$ (i.e. λ is not a Steklov eigenvalue) then $E^s = -E_g$, which is possible only if $E_g = 0$ (i.e $g = 0$) since E^s is outgoing field and E_g is an entire solution of Maxwell's equations.

Thus, with a little more work, for the impedance choice of the auxiliary scattering problem we can state [21]: *The modified far field operator $\mathcal{F}_\lambda$: $L_t^2(\mathbb{S}^2) \to L_t^2(\mathbb{S}^2)$ is injective and has dense range if and only if λ is not a Maxwell's Steklov eigenvalue*

with corresponding eigenfunction W such that $W - E_g$ can be extended outside Ω as an outgoing solution of the homogenous Maxwell's equations. Note that the existence of Steklov eigenvalues in the case of zero absorption is proved in [22].

Our point of view in [21] is that, to avoid the non-compactness of the electromagnetic Neumann-to-Dirichlet operator, we can perturb the rather arbitrary choice of the standard impedance boundary condition to obtain a mathematically simpler eigenvalue problem that can be analyzed using more standard techniques than those in [22]. In particular, one may replace the boundary condition in (10) by

$$\nu \times \operatorname{curl} Q - \lambda \mathcal{S} \left[\nu \times (Q \times \nu) \right] = 0 \qquad \text{on } \partial\Omega$$

where $\mathcal{S}$ is an appropriately chosen regularizing linear operator defined on surface tangential fields on $\partial\Omega$. This change now leads to the eigenvalue problem

$$\operatorname{curl} \mu^{-1} \operatorname{curl} W - k^2 \left(\epsilon_r + \tfrac{i}{k}\sigma_r \right) W = 0 \quad \text{in } \Omega$$
$$\nu \times \mu^{-1} \operatorname{curl} W - \lambda \mathcal{S} \left[\nu \times (W \times \nu) \right] = 0 \quad \text{on } \partial\Omega. \text{(11)}$$

We refer the reader to [21] for a possible choice of the operator $\mathcal{S}$ that defines the above problem as an eigenvalue problem for a compact (and self-adjoint if $\sigma_r = 0$) operator. Roughly, this operator maps surface tangential fields on Ω to tangential fields with zero surface divergence. For numerical results with this operator see [21]. We term these eigenvalues generalized Steklov eigenvalues.

However, in our intended applications of nondestructive evaluation, many materials have a significant level of absorption, i.e. $\sigma_r \neq 0$, hence one deals with non-selfadjoint (non-Hermitian) eigenvalue problems. In a further extension of the impedance type technique [23], one of the authors developed a modification of $\mathcal{S}$ in [21], in which $\mathcal{S} := \mathcal{S}_\delta$ is a smoothing operator with a positive smoothing parameter δ allowing for the use of the theory of trace class operators to show that infinitely many eigenvalues of this new problem exist for an absorbing material whenever δ is sufficiently large. More specifically, since $\partial\Omega$ is simply connected, every square integrable tangential field $\xi \in L^2_t(\partial\Omega)$ can be expressed as

$$\xi = \sum_{m=1}^{\infty} \left[\xi_m^{(1)} \nabla_{\partial\Omega} Y_m + \xi_m^{(2)} \operatorname{curl}_{\partial\Omega} Y_m \right]$$

where $\{Y_m\}_{m=0}^{\infty}$ is the orthonormal basis of $L^2(\partial\Omega)$ consisting of the eigensystem (λ_m, Y_m) of the nonnegative Laplace-Beltrami operator, i.e.

$$\Delta_{\partial\Omega} Y_m = \lambda_m Y_m, \qquad m \geq 0.$$

Then the smoothing operator $\mathcal{S}_\delta$ is defined as

$$\mathcal{S}_\delta \xi := \sum_{m=1}^{\infty} \lambda_m^{-\delta} \xi_m^{(2)} \operatorname{curl}_{\partial\Omega} Y_m.$$

We refer to the eigenvalues (11) with $\mathcal{S} := \mathcal{S}_\delta$ as δ-Stekloff eigenvalues. In particular $\mathcal{S}_0$ coincides with $\mathcal{S}$ chosen in [21], and as $\delta \to 0^+$ the set of δ-Stekloff eigenvalues converges to electromagnetic Stekloff eigenvalues in [21]. The nonnegative parameter δ describes the degree of smoothing, i.e. the order of decay of the singular values of this compact operator. Applying Lidski's Theorem for the trace class operators, one can show that for $\delta > 1$ there exists an infinite set of δ-Stekloff eigenvalues with ∞ as the only accumulation point. For $\sigma_r \neq 0$ δ-Stekloff eigenvalues are complex. Stability analysis of these eigenvalues with respect to changes in the anisotropic electric permittivity can be found in [23]. As yet the use of δ-Steklov eigenvalues has not been tested numerically.

It was shown in [21] that generalized Steklov eigenvalues can be detected from the behavior of the solution of the far field equation

$$\mathcal{F}_\lambda g(\hat{x}) = E^e_\infty(\hat{x}; z, q, k), \qquad z \in D, \qquad (12)$$

where

$$E^e_\infty(\hat{x}; z, q) = \frac{ik}{4\pi} (\hat{x} \times q) \times \hat{x} \, e^{-ik\hat{x}\cdot z}$$

is the far field pattern of the electric dipole

$$E^e(x; z, q) := \frac{1}{4\pi k^2} \operatorname{curl} \operatorname{curl} \frac{e^{ik|x-z|}}{|x-z|} q, \quad q \in \mathbb{R}^3$$

having artificial polarization q and originating at a source point z. More specifically, for *any sequence* $g^\epsilon_z \in L^2_t(\mathbb{S}^2)$ *satisfying*

$$\lim_{\epsilon \to 0} \|\mathcal{F}_\lambda g^\epsilon_z - E^e_\infty(\cdot; z, q)\|_{L^2_t(\mathbb{S}^2)} = 0 \qquad (13)$$

$\|E_{g^\epsilon_z}\|_{L^2(D)}$ *is bounded for all z in ball $B \subset D$ if and only if λ is not a Steklov eigenvalue (of any of the three types mentioned above, assuming they exist), where $E_{g^\epsilon_z}$ is the electric Herglotz wave function with kernel g^ϵ_z.*

The above result suggests that if $g_{z,\alpha}$ is the solution of the regularized far field equation with regularization parameter $\alpha > 0$, i.e. the solution of

$$(\alpha I + \mathcal{F}^*_\lambda \mathcal{F}_\lambda) g = \mathcal{F}^*_\lambda E^e_\infty(\hat{x}, z, q), \qquad (14)$$

with $\mathcal{F}^*_\lambda$ denoting the adjoint of $\mathcal{F}_\lambda$, then varying $z \in B \subset D$ the Steklov eigenvalues will coincide with those values of λ where $\max_z \|E_{g_{z,\alpha}}\|_{L^2(D)}$ or (as is mostly used in practice) $\max_z \|g_{z,\alpha}\|_{L^2_t(\mathbb{S}^2)}$ becomes large. For more mathematical details and preliminary numerical experiments see [21].

It becomes now clear within the framework introduced in this section that new modifications of the far field operator can be introduced based on other choices of the computed auxiliary scattering problem, which will generate new sets of eigenvalues. In the case of Steklov, generalized Steklov and δ-Steklov eigenvalues, these can

be determined from the measured scattering data at a fixed frequency and can thus generate target signatures to identify changes in the medium. The big question is which kind of eigenvalues are more sensitive to what changes in the medium, and a general answer to this question is not currently known.

In the next section we introduce another class of eigenvalues called the *modified transmission eigenvalue* problem, which features an adjustable parameter that might be used to tune the method. These eigenvalues will be used for the numerical tests in this paper.

C. A Modified Transmission Eigenvalue Problem

To define the *modified transmission eigenvalue* problem suggested in [24] we consider the auxiliary scattering problem (which we precompute before processing the measured data): Given the electric incident plane wave $E^i := E^i(\cdot; d, p)$, find the total vector field Q, the scattered vector field Q^s, and a scalar field q with $\int_\Omega q \, dx = 0$ satisfying

$$
\begin{aligned}
\operatorname{curl} \operatorname{curl} Q^s - k^2 Q^s = 0 & \quad \text{in } \mathbb{R}^3 \setminus \overline{\Omega} \\
\operatorname{curl} \gamma^{-1} \operatorname{curl} Q - k^2 \eta Q + k^2 \nabla q = 0 & \quad \text{in } \Omega \\
\nabla \cdot Q = 0 & \quad \text{in } \Omega \\
\nu \cdot Q = 0 & \quad \text{on } \partial\Omega \quad (15) \\
\nu \times Q - \nu \times Q^s = \nu \times E^i & \quad \text{on } \partial\Omega \\
\nu \times \gamma^{-1} \operatorname{curl} Q = \nu \times \operatorname{curl}(E^i + Q^s) & \quad \text{on } \partial\Omega \\
\lim_{|x| \to \infty} (\operatorname{curl} Q^s \times x - ik|x|Q^s) = 0 &
\end{aligned}
$$

where the fixed real parameter $\gamma \neq -1$ is nonzero and $\eta \in \mathbb{C}$ is a complex number that will serve as an eigenvalue parameter. Note that the appearance of the additional scalar field q restores ellipticity in the above transmission problem, which is a great mathematical convenience when we study the eigenvalue problem that it generates.

As explained earlier, we view our unknown inhomogeneity as situated in an artificial background described by this scattering problem. In particular $\gamma < 0$ corresponds to a metamaterial artificial background. For $Q_\infty^\eta(\hat{x}; d, p, k)$ being the far field of the scattered field Q^s, we consider the corresponding modified far field operator $\mathcal{F}_\eta$ defined by (9) (with λ replaced by η). The same analysis of the mathematical properties (injectivity) of $\mathcal{F}_\eta$ as discussed in Section III-A generates the following *modified transmission eigenvalue problem*: Find nontrivial vector fields W and V and a scalar field v

with $\int_\Omega v \, dx = 0$ satisfying

$$
\begin{aligned}
\operatorname{curl} \mu^{-1} \operatorname{curl} W - k^2 \left(\epsilon_r + \frac{i}{k} \sigma_r \right) W &= 0 \text{ in } \Omega \\
\operatorname{curl} \gamma^{-1} \operatorname{curl} V - k^2 \eta V + k^2 \nabla v &= 0 \text{ in } \Omega \\
\nabla \cdot V &= 0 \text{ in } \Omega \quad (16) \\
\nu \cdot V &= 0 \text{ on } \partial\Omega \\
\nu \times W - \nu \times V &= 0 \text{ on } \partial\Omega \\
\nu \times \gamma^{-1} \operatorname{curl} W - \nu \times \mu^{-1} \operatorname{curl} V &= 0 \text{ on } \partial\Omega
\end{aligned}
$$

where $\epsilon = \mu = 1$ and $\sigma = 0$ in $\Omega \setminus \overline{D}$.

Definition: *Values of $\eta \in \mathbb{C}$ for which the above modified transmission eigenvalue problem has a nontrivial solution are called* **modified transmission eigenvalues**.

In [24] it is shown that if $\mu = 1$, $\gamma > 0$ and $\gamma \neq 1$ the set of modified transmission eigenvalues is discrete without finite accumulation point. If $\sigma_r = 0$ then all eigenvalues are real and infinitely many exist. For $\sigma_r > 0$ it can be shown that all eigenvalues are complex, but their existence is yet to be proven. In the case when $\gamma < 0$ and $\gamma \neq -1$, the modified transmission eigenvalue problem has better mathematical structure; in particular, if $\sigma_r = 0$ then all but finitely many modified transmission eigenvalues are of one sign and they satisfy a max-min principle which provides monotonicity properties of the eigenvalues in terms of μ_r and ϵ_r. A theoretical study of the modified transmission eigenvalue problem for $\gamma < 0$ is the subject of a forthcoming paper by the present authors.

As for the Steklov problem, from the aforementioned discussion we see that the modified transmission eigenvalues (real and complex) can be determined from a knowledge of the (measured) scattering data $E_\infty(\hat{x}; d, p)$ at a fixed frequency and precomputed far field patterns $Q_\infty^\eta(\hat{x}; d, p)$ for $\hat{x}, d \in \mathbb{S}^2$ and two linearly independent polarizations p.

Definition: *Modified transmission eigenvalues, measured from the far field data, are the set of target signatures using the auxiliary problem in this section.*

In the next section we show numerical procedures for the determination of modified transmission eigenvalues and present numerical examples showing the viability of these eigenvalues as target signatures to detect changes in an anisotropic electromagnetic medium $(\epsilon_r, \mu_r, \sigma_r)$.

IV. NUMERICAL EXPERIMENTS

The numerical experiments in this section serve to illustrate how one class of target signatures, modified transmission eigenvalues, can be detected from far field data. In addition we provide some evidence of the sensitivity of the eigenvalues to changes in the scatterer. While the theory discussed in the preceding sections is applicable to general position-dependent coefficients, we
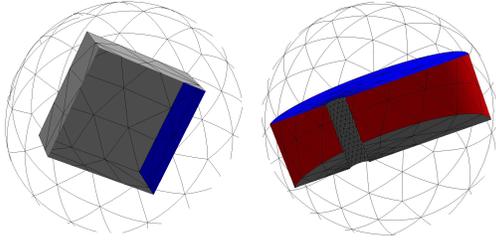
Fig. 2. Scatterers D showing surface meshes for the scattering problem. Left panel: the unit cube D in the unit sphere Ω. Right panel: the damaged puck D inside the unit sphere Ω.

restrict our attention to simple scatterers in which the co-efficients adopt constant values throughout the medium. This approach is intended to lay the groundwork to understand the relationship between the eigenvalues and the medium for more complicated examples that better reflect the types of materials found in a real-world setting. All the results are for synthetic (computed) far field data. For all experiments we use the wavenumber $k = 2$ and we limit ourselves to the dielectric case when $\sigma = 0$.

We limit our study to two scatterers D:

1) The unit cube D centered at the origin (see Fig. 2 left panel).
2) The puck which is a circular cylinder of radius 0.8823 units and height 0.5882 centered at the origin. This "hockey puck" was suggested to us as a simple test scatterer. Holes can be drilled in the puck to represent flaws. For this reason we also consider the "flawed" puck formed from our original puck with a hole of radius 0.08823 centered at a point 0.294 units from the center of the puck and parallel to its axis (see Fig. 2 right panel). The ratio of radius of the puck to height is that of a hockey puck.

For these tests we always take Ω to be the unit sphere which allows us to reuse the auxiliary far field data.

All experiments (except the computation of modified interior eigenvalues for the puck and damaged puck) were run on a Dell desk-side computer having two Intel(R) Xeon(R) Gold 6138 CPUs 2.00GHz and 187 Gbytes of RAM.

The main software components are as follows:

1) **Forward Problem:** We use 4th order Nédélec edge elements of the second kind on tetrahedral elements together with a spherical Perfectly Matched Layer (PML) to approximate (5) in the standard way. This is implemented in Python 3 using the NGSpy front end to Netgen [25]. The mesh is generated using a requested mesh size of $h = $ $2\pi/(4k)$, and the PML is taken to start at radius $2 + 2\pi/k$ and be of thickness $\pi/(2k)$ with Netgen PML parameter set to $2\sqrt{-1}$. Curved boundaries are approximated by 5th order polynomials.

2) **Auxiliary problem:** In order to have a rapid scheme for computing the far field pattern of the auxiliary problem (15) we assume that Ω is the unit sphere for all experiments and use a standard Mie series approach as given in [24]. This is implemented in Matlab (version 2020a).

3) **Modified transmission eigenvalues:** To check that our predicted eigenvalues are true eigenvalues and monitor missing eigenvalues we also solve the transmission eigenvalue problem (16). We again use Netgen/NGSpy to approximate this problem, however the formulation given in (16) is not convenient for implementation. Instead we introduce a new variable $\tilde{W} = W - V$ which has the advantage of a homogeneous boundary condition on $\partial\Omega$. We then reformulate the problem in terms of $\tilde{W}$ and V. The resulting equations are discretized using a Lagrange multiplier to enforce the divergence-free condition and quartic edge elements. The mesh is chosen to have mesh size $h = 2\pi/(4k)$. Eigenvalues are computed using the Arnoldi method with 160 vectors. Typically the computation of eigenvalues is more memory intensive than for the forward problem and limits the maximum wavenumber we can consider.

4) **The modified far field equation:** The far field patterns E_∞ and Q_∞^η are computed using measurement and incident directions at the vertices of an unstructured mesh of $\mathbb{S}^2$ found using Netgen (and for two orthogonal polarizations). We considered two cases: a) a mesh with element size of 0.4 which resulted in a mesh with 99 vertices and b) a mesh with element size of 0.3 which resulted in a mesh with 161 vertices. If N_f denotes the number of vertices on the unit sphere we thus have $2N_f$ far field patterns recorded at the N_f measurement directions. Each far field pattern has two independent polarizations (being tangential to $\mathbb{S}^2$) and so the measurements of the scattering data and auxiliary data result in a $2N_f \times 2N_f$ matrix $\mathbb{F}$ computed from $E_\infty - Q_\infty^\eta$. We then find an approximation to g, denoted $\vec{g}$, at the vertices of the surface grid by solving a matrix version of the Tikhonov regularized problem (14). We use a constant regularization parameter $\alpha = 10^{-8}$, all three independent auxiliary polarizations, and 10 randomly chosen auxiliary source points z inside $[-1/5, 1/5]^3$.

Having found $\vec{g}$ for each source point and source polarization, we average the L^2 norm of the sur-

face function defined by $\vec{g}$, and then use this quantity to detect target signatures by graphing the average norm of $\vec{g}$ against the eigenvalue parameter η. Peaks in this graph should signal modified transmission eigenvalues. Obviously the parameters used here would have to be modified for different wave numbers and different scattering experiments.

The most time-consuming part of this algorithm is the calculation of the far field pattern of the auxiliary problem (15). This must be done for a dense discrete set of η in the interval where the modified transmission eigenvalues are sought. However, fixing the auxiliary domain Ω to be the unit sphere means this only needs to be done once in an offline stage for each different choice of k, η and far field grid (independently of the scatterer provided it fits in Ω). Moreover, for the sphere we can use a Mie series as pointed out above. In practice the far field pattern of the forward scattering problem would be measured, and so it remains to solve the discrete far field equation for each source point z and polarization q. In our study using 161 source and points and 1701 values of η this procedure took approximately 582 seconds which includes the time-consuming need to read in large text data files.

A. The unit cube

We start by investigating target signatures for a simple unit cube. We choose $\mu = 1$ and $\epsilon = 2$ in the cube (except when we consider an anisotropic scatterer later in this section) and take Ω to be the unit ball. In Fig. 3 we show the "exact" modified transmission eigenvalues computed by our finite element code as stars along the x-axis. Using 99 incoming directions and measurements results in a poor approximation of some the eigenvalues (the eigenvalues around $\eta = 12$ in particular). Such inaccuracy can be due to excessive noise, or an insufficiently resolved calculation, but in this case we tested adding more directions. From the figure it appears that a choice of 161 directions results in an improved agreement between peaks and eigenvalues, with the exception of one eigenvalue that is not detected in either case by the LSM approach. We use this number of directions in all remaining simulations, recognizing that a sufficient number may depend on the geometry of the scatterer. There is not yet a rule of thumb for how many directions are needed for a given problem.

Next we investigate the sensitivity of eigenvalues to changes in bulk ϵ for a homogeneous isotropic cube. As ϵ varies, the eigenvalues shift. The magnitude of the shift depends on index of the eigenvalue, as well as the choice of the auxiliary parameter γ. In Fig. 4 we track two eigenvalues when $\gamma = 0.5$, and Fig. 5 is
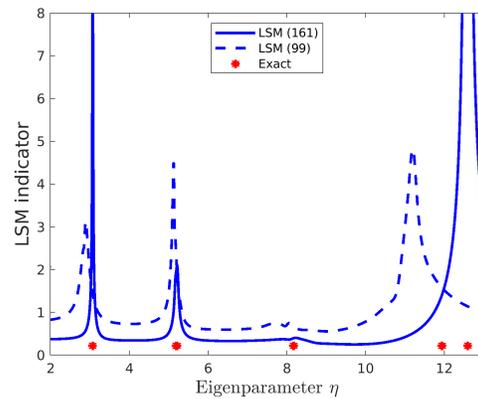
Fig. 3. Detection of eigenvalues for an isotropic cube with $\gamma = 0.5$, 2% relative noise, and both 99 (dashed curve) and 161 (solid curve) incident directions.
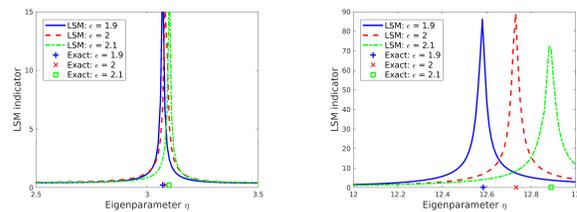
Fig. 4. The change in eigenvalues due to changes in the scatterer depends on the eigenvalue (and on the nature of the change). Here we track two eigenvalues as ϵ varies. The eigenvalue tracked in the left panel has a small change, whereas the eigenvalue in the right panel shows significant sensitivity to changes in ϵ. These results are for an isotropic cube with 161 incident directions, $\gamma = 0.5$, and 2% relative noise.

the corresponding result when $\gamma = 2$. In both cases we consider $\epsilon = 1.9, 2, 2.1$. Comparing the two results, it is clearly beneficial to use $\gamma = 0.5$ and use the eigenvalue near $\eta = 12.7$ to detect changes in ϵ. Of course, a good choice of γ and an eigenvalue to consider likely depends on the scatterer of interest. In particular, an optimal choice of γ has not been determined.

One interest in target signatures is to detect changes

(a)   (b)
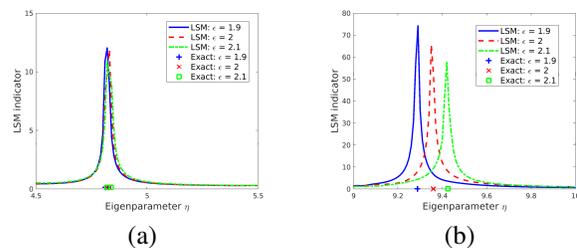
Fig. 5. A similar result to that in Fig. 4 but for the choice $\gamma = 2$. This choice of γ provides less sensitivity to the changes in ϵ compared to $\gamma = 0.5$.
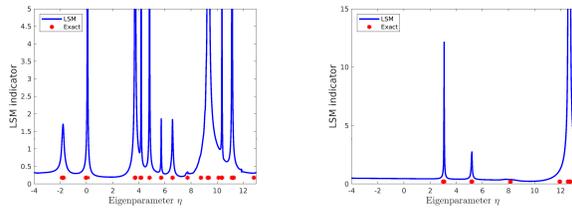
Fig. 6. Detection of eigenvalues for an anisotropic cube with 161 incident directions, Left: $\gamma = 2$. Right: $\gamma = 0.5$. Both have 2% relative noise on the data.
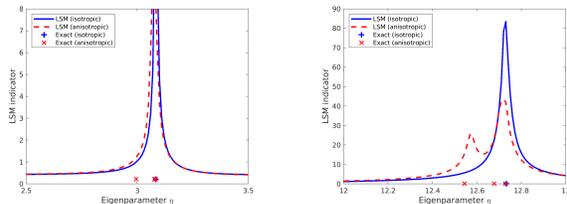
Fig. 7. Indicator function plots for an isotropic cube and an anisotropic cube with 161 incident directions, $\gamma = 0.5$, and 2% relative noise.

Fig. 8. Indicator function plots for an isotropic "unflawed" puck and a "flawed" puck-with-a-hole using 161 incident directions, $\gamma = 2$, and 2% relative noise.

in anisotropic scatterers. If ϵ and μ are allowed to be general symmetric positive definite matrix functions of position, it is not possible to reconstruct ϵ and μ from far field measurements (the discussion in [12] carries over to Maxwell's equations directly). Changes in target signatures could detect changes in anisotropy. To initiate an investigation of this idea, we compare target signatures for $\mu = 1$ and $\epsilon = 2$ with those of an anisotropic scatterer with

$$
\epsilon = \begin{pmatrix} 1.9 & 0 & 0 \\ 0 & 2 & 0 \\ 0 & 0 & 2 \end{pmatrix}, \quad \mu = \begin{pmatrix} 1 & 0 & 0 \\ 0 & 1 & 0 \\ 0 & 0 & 0.9 \end{pmatrix}.
$$

In Fig. 6 we show the determination of modified interior transmission eigenvalues for the anisotropic cube. Clearly we can determine an approximation to several eigenvalues from scattering data, and the spectrum for $\gamma = 0.5$ is simpler than that for $\gamma = 2$.

Next in Fig. 7 we show the displacement of the eigenvalues for the isotropic and anisotropic cube. As for the isotropic case, some eigenvalues are more sensitive than others. Interestingly , the anisotropy splits the multiple eigenvalue at approximately $\eta = 12.7$ (see the right hand panel). One of these is not picked up from the far field pattern.

B. The hockey puck

It has been suggested to us that a hockey puck would be a useful experimental dielectric scatterer. In this example we consider a puck shaped dielectric scatterer with $\mu = 1$ and $\epsilon = 2$. We consider the "unflawed"

isotropic puck and the "flawed" puck with a hole drilled through it. The graph of the indicator function against η is shown in Fig. 8. Note that the location of predicted eigenvalues moves as a result of this flaw. We are unable to verify the exact eigenvalues due to limitations in our software (we are unable to refine the mesh sufficiently to capture all eigenvalues accurately), but the result is encouraging in that it shows that the scheme can detect flaws of this type and not just bulk changes in ϵ. Of course, limitations due to numerical computations of the forward problem or eigenvalues do not reflect any limitation on finding target signatures from measurements, since there is no need to solve the direct problem to obtain target signatures.

V. CONCLUSION

We have described new classes of target signatures based on eigenvalue problems. We have demonstrated that one class, modified transmission eigenvalues, may be determined from single frequency data using multistatic measurements. We have also shown examples of how simple flaws or changes in electromagnetic properties cause the eigenvalues to shift. At this stage it would be very interesting to try to use experimental data to determine modified transmission eigenvalues from far field data.

ACKNOWLEDGMENT

REFERENCES

[1] X. Chen, Computational Methods for Electromagnetic Inverse Scattering. Wiley-IEEE Press, 2018. M. Pastorino and A. Randazzo, Microwave Imaging Methods and Applications. Artech House, 2018.

[2] K. Belkebir and M. Saillard, "Special section: Testing inversion algorithms against experimental data," Inverse Problems, vol. 17, no. 6, pp. 1565–1571, Nov. 2001.

[3] K. Belkebir and M. Saillard, "Testing inversion algorithms against experimental data: Inhomoge- neous targets," Inverse Problems, vol. 21, no. 6, S1–S3, Dec. 2004.

[4] A. Litman and L. Crocco, "Testing inversion algorithms against experimental data: 3D targets," Inverse Problems, vol. 25, no. 2, p. 020 201, Feb. 2009.

[5] O. Dorn and D. Lesselier, "Introduction to the special issue on electromagnet inverse problems: Emerging methods and novel applications," Inverse Problems, vol. 26, no. 7, p. 070 201, Jul. 2010. L. Di Donato and A. F. Morabito, "Special issue "microwave imaging and electromagnetic inverse scattering problems"," Journal of Imaging, vol. 5, 2019.

[6] G. Bao and P. Li, Inverse medium scattering problems for electromagnetic waves, SIAM J. Appl. Math., Vol 65 (2006), 2049-2066.

[7] T. Hohage and F. Weidling, Verification of a variational source condition for acoustic inverse medium scattering, Inverse Problems, Vol. 31 (2015), 075006.

[8] F. Cakoni, D. Colton, and P. Monk, The Linear Sampling Method in Inverse Electromagnetic Scattering, CBMS-NSF Regional Conference Series in Applied Mathematics. Philadelphia: SIAM, 2011, vol. 80.

[9] H. Houssem, R. Hiptmair, P. Monk, and R. Rodríguez, Computational electromagnetism, Lecture Notes in Mathematics, 2148, Fondazione CIME/CIME Foundation Subseries. Springer, 2016, notes from the CIME School held in Cetraro, June 9?14, 2014. Edited by A. Bermúdez de Castro and A. Valli.

[10] M. Burnfeindt and H. Alqadah, "Enhancement of linear sampling method imaging of conducting targets using a boundary condition constraint," 2020 IEEE Research and Applications of Photonics in Defense Conference (RAPID), 2020.

[11] L. Audibert, F. Cakoni, and H. Haddar, New sets of eigenvalues in inverse scattering for inhomogeneous media and their determination from scattering data, Inverse Problems, Vol. 33, 125011, 2017.

[12] F. Gylys-Colwell, An inverse problem for the Helmholtz equation, Inverse Problems vol. 12, pp. 139-156, 1996.

[13] C. Baum. The Singularity Expansion Method in Electromagnetics: a Summary Survey and Open Questions, Lulu Enterprises, 2012.

[14] S. Dyatlov and M. Zworski, Mathematical Theory of Scattering Resonances, AMS Graduate Studies in Mathematics, 200, American Mathematical Society, Providence, 2019.

[15] L. Audibert , L. Chesnel, H. Haddar, and K. Napal, Qualitative Indicator Functions for Imaging Crack Networks Using Acoustic Waves SIAM J. Sci. Comput., 43 (2021), B271–B297.

[16] P. Monk, Finite Element Methods for Maxwell's Equations. Oxford: Oxford University Press, 2003.

[17] L. Audibert, L. Chesnel, and H. Haddar, Transmission eigenvalues with artificial background for explicit material index identification, C. R. Math. Acad. Sci. Paris, Vol. 356, pp. 626–631, 2018.

[18] D. Colton and R. Kress, Inverse Acoustic and Electromagnetic Scattering Theory, 4rth ed. New York: Springer-Verlag, vol 93, 2019.

[19] F. Cakoni, D. Colton and P. Monk, Qualitative methods in inverse electromagnetic scattering theory, IEEE Antennas and Propagation Magazine, 24-33, October Issue, 2017.

[20] S. Cogar, D. Colton, and P. Monk, Eigenvalue problems in inverse electromagnetic scattering theory, in Maxwell's Equations, U. Langer, D. Pauly, and S. Repin, eds., no. 24 in Radon Series on Computational and Applied Mathematics, De Gruyter, pp. 145–169, 2019.

[21] J. Camanõ, C. Lackner, and P. Monk, Electromagnetic Stekloff eigenvalues in inverse scattering, SIAM J. Math. Anal. Vol. 49, pp. 4376–4401, 2017

[22] M. Halla, Electromagnetic Stekloff eigenvalues: existence and behavior in the selfadjoint case, arXiv:1909.01983, 2019.

[23] S. Cogar, Existence and stability of electromagnetic Stekloff eigenvalues with a trace class modification, arXiv:2006.16428, to appear in Inverse Problems and Imaging.

[24] S. Cogar and P. Monk, Modified electromagnetic transmission eigenvalues in inverse scattering theory, arXiv:2005.14277, to appear in SIAM J. Math. Anal.

[25] Netgen/NGSolve multiphysics finite element software available from https://ngsolve.org.

Fioralba Cakoni (fc292@math.rutgers.edu) is a distinguished professor in the Department of Mathematics at Rutgers University, New Brunswick. She is co-author of *The Linear Sampling Method in Inverse Electromagnetic Scattering* (CBMS-SIAM 2011) with D. Colton and P. Monk, co-author of *A Qualitative Approach to Inverse Scattering Theory* (Springer, 2014) with D. Colton, and of *Inverse Scattering Theory and Transmission Eigenvalues* (CBMS-SIAM 2016) with D. Colton and H. Haddar.

Samuel Cogar (sc2083@math.rutgers.edu) is a Hill assistant professor in the Department of Mathematics at Rutgers University, New Brunswick.

Peter Monk (monk@udel.edu) is a Unidel professor in the Department of Mathematical Sciences at the University of Delaware. He is the author of *Finite Element Methods for Maxwell's Equation* and co-author with F. Cakoni and D. Colton of *The Linear Sampling Method in Inverse Electromagnetic Scattering* (CBMS-SIAM 2011).